

## RESEARCH ARTICLE

# An Improved Feature Extraction Method for Surface Electromyography Based on Muscle Activity Regions

LUYAO MA<sup>1</sup>, QING TAO<sup>1</sup>, QINGZHENG CHEN, AND ZIRUI ZHAO

School of Mechanical Engineering, Xinjiang University, Urumqi 830017, China

Corresponding author: Qing Tao (xjutao@qq.com)

This work was supported in part by the National Natural Science Foundation of China under Grant 51865056, and in part by the National Natural Science Foundation of China-Xinjiang Joint Fund under Grant 2020E0259.

This work involved human subjects or animals in its research. The authors confirm that all human/animal subject research procedures and protocols are exempt from review board approval.

**ABSTRACT** In the analysis of surface electromyography signals (sEMG), the extraction of suitable features is one of the key factors affecting pattern recognition. The aim of this paper is to propose an improved sEMG feature extraction algorithm based on muscle activity regions. The fusion of muscle activity intensity on the basis of muscle activity regions compensates for the low accuracy of the original features for the recognition of similar movements. In this paper, the sEMG signals of five leg movements were collected, including two similar movements: upstairs and downstairs, standing and sitting. The classification performance of the features before and after the improvement was tested with six classifiers. It proves that the new characteristic, active muscle position and intensity (AMPI), greatly improves the classification accuracy of similar movements. The paper also compares the new features with the traditional eight classification features. The results show that the new features are at the forefront of the classification performance, with a very small difference in classification accuracy of 4.1% compared to the best performing features. This confirms the high practical value of the new features. New features are still based on the mapping relationship between movement patterns and active muscle regions. This provides new ideas for the feature extraction method of sEMG signals. In addition, compared with the traditional features, the new feature still have the ability to reduce the dimension, which provides a more applicable feature extraction method for the application of multi-channel electromyogram (EMG) signals acquisition devices and high-density electrodes.

**INDEX TERMS** Surface electromyography signals, feature extraction, active muscle regions, similar movements, pattern recognition.

## I. INTRODUCTION

In recent years, electromyogram (EMG) signals, are widely used in the identification of human movement intention, which is an important way to achieve a flexible and friendly human-computer interaction environment [1]. EMG signals are signals that record and analyze the electrical activity generated by muscle contractions [2]. They are useful electrophysiological signals which are non-stationary, non-linear, and high complex signals and carry the distinct

The associate editor coordinating the review of this manuscript and approving it for publication was Taous Meriem Laleg-Kirati<sup>1</sup>.

signature of voluntary intent of central nervous system [3]. EMG signals are classified as invasive or surface EMG according to the placement of the measurement electrodes, surface electrodes are widely used due to their non-invasive nature [4]. Surface electromyography (sEMG) is widely used in the fields of exoskeleton control, muscle fatigue and contraction measurement, ergonomics and human-computer interaction [5], [6].

The control of lower limb exoskeleton robots is an important aspect of the application of surface electromyogram signal. With the continuous development of the lower limb exoskeleton robot, it has become an assisted walking

device that incorporates mechanical, sensing and control technologies [7]. It is widely used in many fields such as military, medical and aviation [8], [9]. Such as: BLEEX [10], ReWalk [11], skeletal rehabilitation robots [12] and Space remote robot [13]. The key issue in lower limb exoskeleton research is to achieve precise perception of the wearer's movement intentions and achieve the coordination of man-machine movements. Many researchers have used EMG signals for motor intent recognition and exoskeleton control. Feature extraction is a key step in achieving accurate intention recognition and developing flexible control strategies [14], [15]. Researchers have made many efforts in this area. Such as: Region-Cable News Network and wavelet feature extraction methods [16], feature extraction methods based on minimum entropy deconvolution adjustment [17], feature extraction methods based on multi-method integration combining wavelets, fractals and statistics [18] and feature extraction methods based on improved small-world leaky echo state networks [19].

Gongfa Li et al. proposed a feature named activity muscle regions (AMR) in 2019 [20]. The feature is based on the mapping relationship between limb movements and active muscle regions. This feature has been applied to hand motion recognition and good classification results have been obtained. However, the feature does not work well for classifying similar movement patterns. The core of limb movement is joint movement, and different joint movements constitute different movement patterns. For limb movements, the number of joints is limited while the variety of movements is immeasurable. For leg movements in particular, there are only three leg joints: hip, knee and ankle, but the resulting leg movement patterns are not limited to walking, running, upstairs and downstairs, etc. It is therefore likely that different movement patterns call for the same movement joints. Different muscle contractions drive different motor joints. Therefore, the same motor joint means that the active muscles are the same. This imposes significant limitations on the classification performance of muscle activity regions (AMR). To address this issue, this paper introduces muscle activity intensity on the basis of muscle activity regions. The fusion of the two types of information constitutes a new feature, namely the Active Muscle Position and Intensity (AMPI). Five leg movement patterns were tested for classification using new features. The new features show better classification of similar leg movements compared to the activity muscle regions (AMR) before the improvement. This paper also compares the improved new features with the traditional eight features. The experimental results show that the new feature still has good classification performance compared with the commonly used classification features. This proves that the new features have high utility in motion pattern recognition.

The rest of the paper is organized as follows. Section II describes the experimental data acquisition method and the signal processing methods. Section III provides an improved feature extraction method. Section IV discusses the



FIGURE 1. The EMG acquisition equipment.

performance evaluation programme in detail. The experimental results are analyzed in section V. Finally, section VI reaches conclusions and discusses future directions for the work.

## II. sEMG SIGNALS COLLECTION

Eight subjects took part in this experiment, five men and three women, aged between 20 and 30 years. The subjects were physically healthy and had no neurological or muscular disorders. Before participation, all subjects agreed to participate in this study and were briefed about the experiment.

The sEMG is typically collected by one or more electrodes placed on the surface of the skin. The distribution of electrodes and the position of the attachment point can significantly affect the accuracy of the recognition of movement patterns [21]. As shown in Figure 1, The EMG acquisition equipment from PLUX in Portugal was used to collect the experimental data. In order to obtain better skin impedance, the subject must wash the skin of the leg with alcohol before the experiment [22]. In this paper, the sEMG sampling frequency is set to 1 kHz, which is twice the maximum frequency, consistent with the Nyquist sampling theorem.

In total, five sEMG signals for common leg movements were collected for each subject. The five movements are walk, upstairs, downstairs, stand and sit. The experimental scenario is shown in Figure 2. Each action was repeated 10 times.

The muscles in each joint of the body are divided into extensor and flexor muscles according to the different modes of action. When selecting the test point, the larger or longer of the human lower limb muscles should be chosen in order to make the experiment simple and easy to perform. In this way, the test point has good discrimination, which will not lead to errors in the subsequent experiment due to the position deviation of the electrode patch. Through in-depth analysis of the production mechanism of human lower limb action and the function of the muscle group, the six muscles of the human lower limb, namely Medial and



**FIGURE 2.** Diagram of the experimental scenarios (walk (1), upstairs (2), downstairs (3), sit (4), stand (5)).

lateral femoral muscles of the quadriceps, Biceps femoris, the tibialis anterior muscle on the calf, the medial head and the lateral head of gastrocnemius, were selected as the sEMG signal acquisition points for the five movement patterns of the human lower limb. As shown in Figure 3.

During the experiment, each movement was repeated 10 times in 20 seconds and 50 data were collected from each subject. In order to avoid the influence of redundant signals, this paper eliminates all but the active signal, As shown in Figure 4. In this paper, A total of 400 leg movement signals were collected.

As a reflection of the electrophysiological activity of motor nerve cells in the spinal cord in the surface of skeletal muscle, sEMG is essentially a complex physiological signal with non-smooth properties. In the process of picking up and processing of sEMG signals on the skin surface, the interference signal of the internal circuit of the electrode piece and the physiological noise are inevitably intermingled. Therefore, the extracted activity signals need to be denoised with a Butterworth band-pass filter from 50 HZ to 350 HZ and a 50 HZ notch filter before feature extraction [23], [24].

**III. FEATURE EXTRACTION**

The sEMG can assess and record the extent of muscle activity and can also quantify muscle contraction. Different joint movements constitute different movements, while various muscles and muscle contraction degree will cause diverse joint movements. For a movement, the contraction rate of the main active muscle is significantly higher than the others, and the degree of muscle contraction is positively correlated with the strength of the sEMG signal. Different muscles are distributed in different areas of the limb, and the movements of the limb and the main active muscle areas will show a mapping relationship. However, this mapping relationship is not completely one-to-one. For different movements, especially leg movements, the number of muscles is limited, but the type of movements is incalculable. muscle activity regions do not fully characterize all limb movements. Introducing muscle activity intensity based on activity muscle position has a better representation ability for complex and numerous limb movements.

The technique of taking useful information from the input muscle activity signals into a simplified representative set of features is called feature extraction. The results of

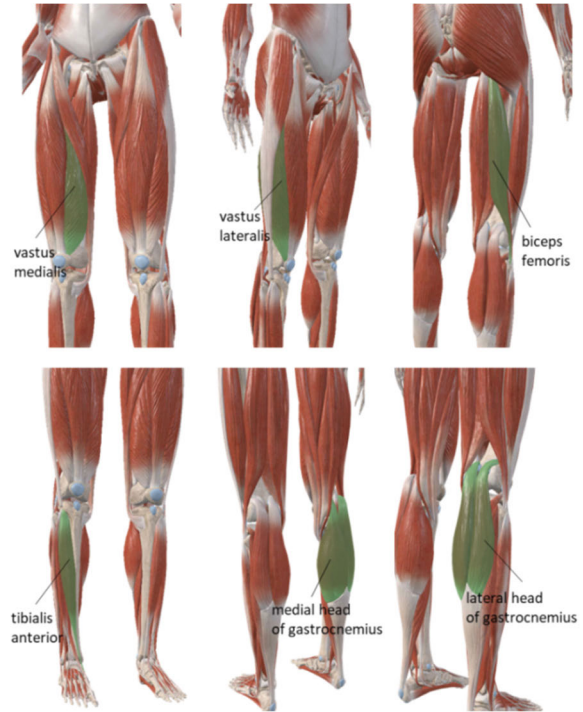


**FIGURE 3.** Diagram of human lower limb muscle selection.

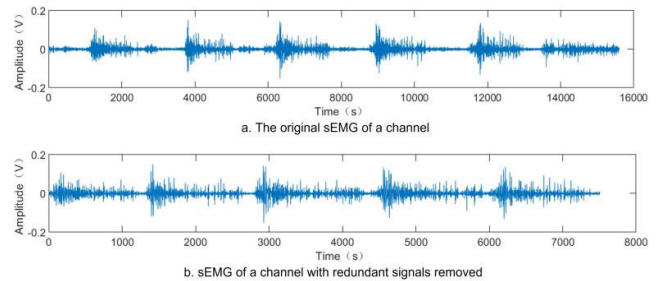


**FIGURE 4.** Removal of redundant signals from sEMG.

classification using sEMG is largely related to the choice of sEMG features. This paper uses windowing techniques to calculate features from sEMG signals, extract temporal features and minimize spectral leakage. The window length determines how many samples will be used for classification recognition, and larger window lengths help to improve identification accuracy. However, there is a trade-off between latency and recognition accuracy [25]. For the above reasons, a moving window algorithm with a 1000ms time window and a 200ms increasing window was used to extract sEMG features.

In this paper, Mean Absolute Value (MAV) is still chosen to extract the main active muscle areas and to define the intensity of muscle activity. The mean absolute value (MAV) is a typical characteristic parameter in the time domain analysis of sEMG signals, which can be used to measure the strength of the surface EMG signal and determine whether the muscle is activated [26]. Calculate the mean absolute value

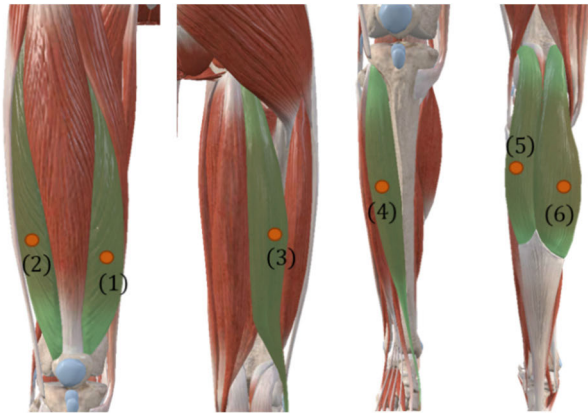


**FIGURE 5.** The position relationship and numbers between the muscle and the electrode.

(MAV) of each leg movement signal. Where  $I$  is the number of sample data segments,  $x_{kj}$  is the  $k$ th sample data in segment  $j$ , and  $N_j$  is the number of samples for this segment. The mean absolute value is defined as (1).

$$\text{MAV}_j = \frac{1}{N_j} \sum_{k=1}^{N_j} |x_{kj}|, j = 1, 2, \dots, I \quad (1)$$

According to the position of the selected muscle and the attachment point of the EMG acquisition device, the position relationship and numbers between the muscle and the electrode are shown in Figure 5. The experimental location deviates less from the actual location.

According to the results of Figure 5, each muscle uses an electrode to measure the muscle activity level and represents it by a number. In this paper, mean absolute values (MAV) were used to quantify muscle activity levels. A sliding time window is used to divide the acquired activity signal into a number of movement signals. The MAV for each channel of each signal is calculated to obtain a set of  $N$  values (the calculation results in a set of 6 values in this paper). These  $N$  values form a set  $X$ , which is shown in (2).

$$X = \{x_1, x_2, \dots, x_N\} \quad (2)$$

The number of the muscle corresponding to each value in set  $X$  constitutes another set  $Y$ . The set is shown in (3).

$$Y = \{y_1, y_2, \dots, y_N\} \quad (3)$$

The elements in the set  $X$  are arranged in order from large to small, and then the  $r$  elements located in front are taken out to form the set  $M_1$ .  $M_1$  is shown in (4). Where  $r$  is the number of active muscles selected, which can be obtained by the analysis of the number of selected muscles and sEMG. As shown in the figure 6, at the same time point, the number of mainly active muscles is about 2 to 4 pieces. In addition, in order to avoid increasing the dimension of composite feature matrix, the  $2r \leq N$  should be guaranteed. Therefore, in this paper,  $r$  is 3.

$$M_1 = \{x_a, x_b, \dots, x_r\} \quad (4)$$

According to  $M_1$ ,  $X$  and  $Y$ , the number of the muscle corresponding to each value in set  $M_1$  can be obtained, which constitutes another set  $M_2$ . As shown in (5).

$$M_2 = \{y_a, y_b, \dots, y_r\} \quad (5)$$

The set  $M$  can be obtained from  $M_1$  and  $M_2$ , which is shown in (6).

$$M = \{(x_a, y_a), (x_b, y_b), \dots, (x_r, y_r)\} \quad (6)$$

In this paper, a vector is obtained by using the 3 elements in the set  $M$ . Thus, a 6 ( $3 \times 2$ )-dimensional feature vector is obtained from the sEMG signal of each frame. This feature based on the main active muscle area and muscle activity intensity is called the active muscle position and intensity (AMPI).

#### IV. PERFORMANCE EVALUATION

The performance evaluation in this paper mainly includes two parts. (1) By verifying the classification performance of the new features against the features before the improvement using six commonly used classifiers. The advantages of using the improved new features in terms of improved classification accuracy are demonstrated. (2) Comparing the new features with the traditional eight classification features, it was verified that the classification performance of the new features is still at the top compared to the commonly used features, proving the usefulness of the new features.

This paper compares the improved new features with the muscle activity region (AMR). Multiple classifiers were used to obtain classification accuracy and evaluate the applicability of new features for leg motion classification. In terms of classifiers, researchers have proposed and applied many methods for handling and distinguishing sEMG signals. Including radial basis function artificial neural networks [27], hidden markov models (HMMs) [28], gaussian mixture models (GMMs) [29], [30], fuzzy methods [31] and support vector machines (SVM) [32]. In this study, six classifiers, support vector machine (SVM), k-nearest neighbor (KNN), The classification and regression tree (CART), back propagation neural network (BP), random forest (RF) and linear discriminant analysis (LDA), were selected for classification and identification. Matlab software was used for the signal processing and feature extraction steps, and then the extracted data was classified. Results of the classifier were evaluated using a 5-fold cross-validation. Classification accuracy is used as the main metric to evaluate the classification performance of the new features.

In this study, the improved new features are compared with the commonly used time domain, frequency domain, and nonlinear features. Traditional feature sets including root mean square (RMS), variance (VAR) and zero crossing (ZC) in the time domain; median frequency (MF) and mean power frequency (MPF) in the frequency domain; approximate entropy (ApEn), fuzzy entropy (FuzzyEn) and lempel-ziv complexity (LZC) for non-linearities.

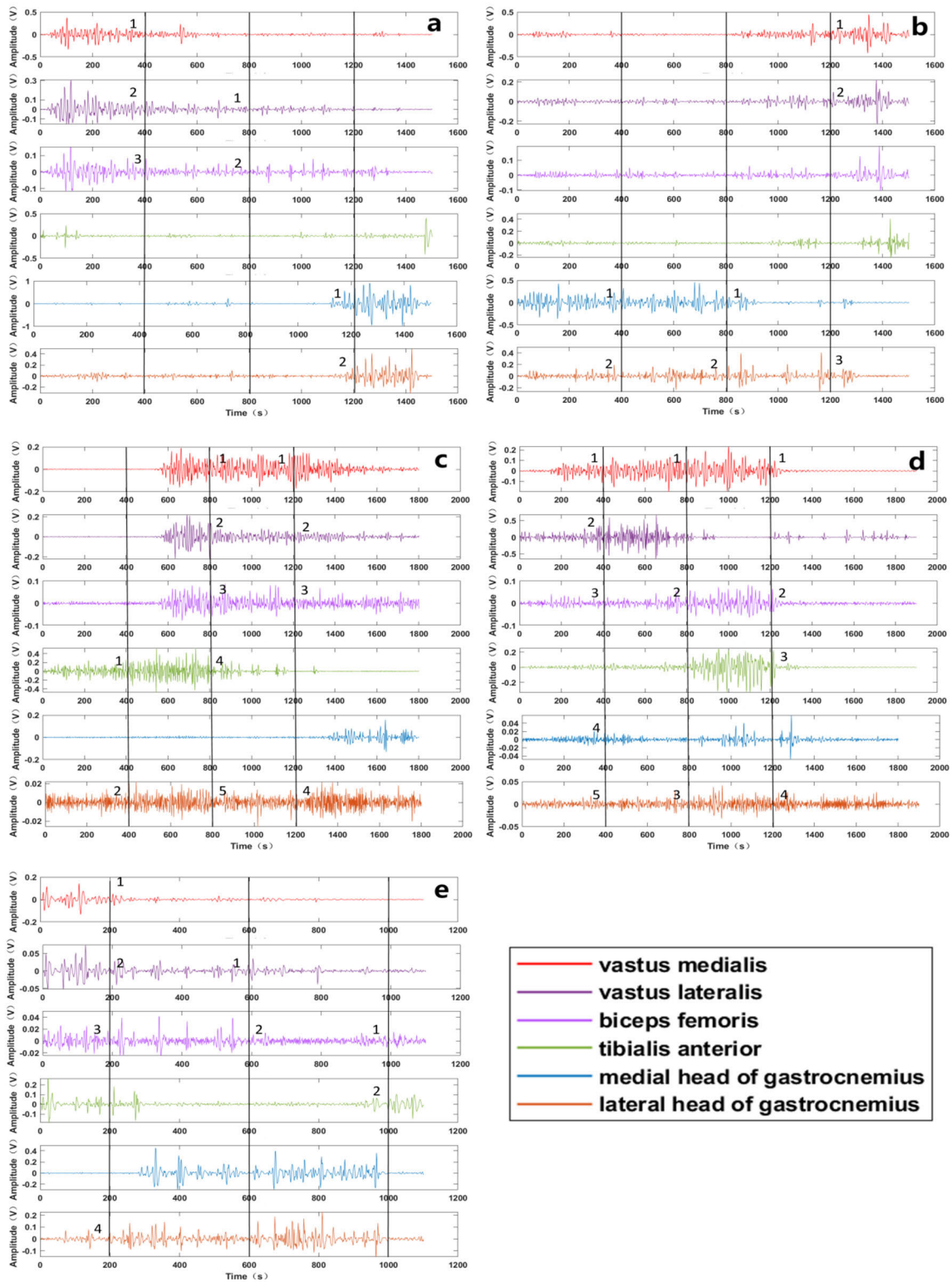


**FIGURE 6.** Diagram of activity signals in different movement modes (upstairs (a), downstairs (b), sit (c), stand (d), walk (e)).

Root mean square (RMS), the root mean square value of all amplitudes over a period of time, characterizes the average

variation in sEMG over time. Where  $x_i(i=1, 1, 2, \dots, N)$  is a time series of length  $N$ . The root-mean-square value is

defined as (7).

$$\text{RMS} = \sqrt{\frac{1}{N} \sum_{i=1}^N x_i^2} \quad (7)$$

Variance (VAR), the degree to which a sample deviates from the mean, reflects the trend in the degree of dispersion of the sEMG signal. Where  $x_i (i=1, 1, 2, \dots, N)$  is a time series of length  $N$ , and  $\bar{x}$  represents the mean of the signal of length  $N$ . The variance is defined as in (8).

$$\text{VAR} = \frac{1}{N-1} \sum_{i=0}^{N-1} [x_i - \bar{x}]^2 \quad (8)$$

Zero crossing (ZC) refers to the number of times the amplitude value of the sEMG crosses the zero y-axis. This feature provides an approximate estimate of the frequency-domain properties. Where  $x_i (i=1, 1, 2, \dots, N)$  is a time series of length  $N$ . The definition is as (9).

$$\text{ZC} = \sum_{i=1}^{N-1} [\text{sgn}(x_i \times x_{i+1}) \cap |x_i - x_{i+1}| \geq \text{threshold}],$$

$$\text{sgn}(x) = \begin{cases} 1, & \text{if } x \geq \text{threshold} \\ 0, & \text{otherwise} \end{cases} \quad (9)$$

Median frequency (MF), the intermediate value of the firing frequency, which is the middle value of the discharge frequency during muscle contraction. Where  $P(f)$  is the power spectral density function of the signal, and  $f_{\text{MF}}$  is the median frequency to be obtained. The definition is as (10).

$$\int_0^{f_{\text{MF}}} P(f) df = \int_{f_{\text{MF}}}^{+\infty} P(f) df = \frac{1}{2} \int_0^{+\infty} P(f) df \quad (10)$$

Mean power frequency (MPF), the average of frequencies over a period of time. Where  $P(f)$  is the power spectral density function of the signal. The average power frequency is defined as (11).

$$f_{\text{MPF}} = \frac{\int_0^{+\infty} fP(f) df}{\int_0^{+\infty} P(f) df} \quad (11)$$

Approximate entropy (ApEn) is a number used to express the complexity of the time series. The more complex the time series, the larger the approximate entropy. It has superior anti-interference capability, especially for the analysis of sEMG. Where  $x_{i=1,1,2,\dots,N}$  is a time series of length  $N$ . With a window of  $m$ , the time series is divided into  $N-m+1$  series.

$$x_i(t) = (x_i(t), x_{i+1}(t), \dots, x_{i+m-1}(t)) \quad (12)$$

Calculate the distance between each sequence and all  $N-m+1$  sequences.

$$d_{ij} = \text{Max} |x_{i+k}(t) - x_{j+k}(t)|, k = 0, 1, \dots, m-1 \quad (13)$$

To define the threshold of  $F = r \times \text{SD}$ . Where  $r = 0.1 \sim 0.25$ ,  $\text{SD}$  is the standard deviation of the sequence.  $C_i^m(t)$  is the

ratio of the numbers in the sequence greater than  $F$  to the total numbers. Based on all  $C_i^m(t)$ , its log average was calculated.

$$\Phi^m(t) = \frac{1}{N-m+1} \sum_{i=1}^{N-m+1} \ln C_i^m(t) \quad (14)$$

Increase the window to  $m+1$  and repeat (12)-(14). The approximate entropy is calculated as (15).

$$\text{ApEn} = \Phi^m(t) - \Phi^{m+1}(t) \quad (15)$$

Fuzzy entropy (FuzzyEn), which uses a fuzzy subordination function to define the similarity of vectors. It exhibits better monotonicity, relative consistency and greater robustness to noise when characterizing signals of varying complexity. Where  $x_i (i=1, 1, 2, \dots, N)$  is a time series of length  $N$ . With a window of  $m$ , the time series is divided into  $N-m+1$  series.

$$x_i(t) = (x_i(t), x_{i+1}(t), \dots, x_{i+m-1}(t)) \quad (16)$$

Calculate the distance between each sequence and all  $N-m+1$  sequences.

$$d_{ij} = \text{Max} |x_{i+k}(t) - x_{j+k}(t)|, k = 0, 1, \dots, m-1 \quad (17)$$

where  $r = 0.1 \sim 0.25$ , the fuzzy membership is calculated by distance  $d$ .

$$D_{ij}^m = \mu(d_{ij}^m, N, r) = \exp\left(\frac{-(d_{ij}^m)^N}{r}\right) \quad (18)$$

Calculate the average of all fuzzy membership except itself.

$$\Phi^m(N, r) = \frac{1}{N-m} \sum_{j=1}^{N-m} \left[ \frac{1}{N-m+1} \sum_{j=1, j \neq i}^{N-m} D_{ij}^m \right] \quad (19)$$

Increase the window to  $m+1$  and repeat (16)-(19). The fuzzy entropy is calculated as (20).

$$\text{FuzzyEn} = \ln \Phi^m(t) - \ln \Phi^{m+1}(t) \quad (20)$$

Lempel-Ziv complexity (LZC) is a method to characterize the rate at which new patterns appear in a time series and is used to measure the rate at which new patterns are added as the time series increases. It can reflect the degree of disorder of the sequence. First, the median value of the time series of the signal is set as a threshold. Time points in the sequence that are greater than the threshold is 1 and time points that are less than the threshold are 0. The time series after binarization is defined as  $S(S_1, S_2, \dots, S_n)$ , where  $n$  is the length of the time series of the signal. The initial value  $C(n)$  of LZC was set to 1. Second, through the time series points to update  $C(n)$ . For each new subsequence occurrence in the time series, the value of  $C(n)$  adds 1, until all sequence points are traversed. Finally, the final  $C(n)$  was normalized. For a sufficiently long random binary sequence, there is defining equation as (21).

$$C(n) = b(n) = \frac{n}{\log_2 n} \quad (21)$$

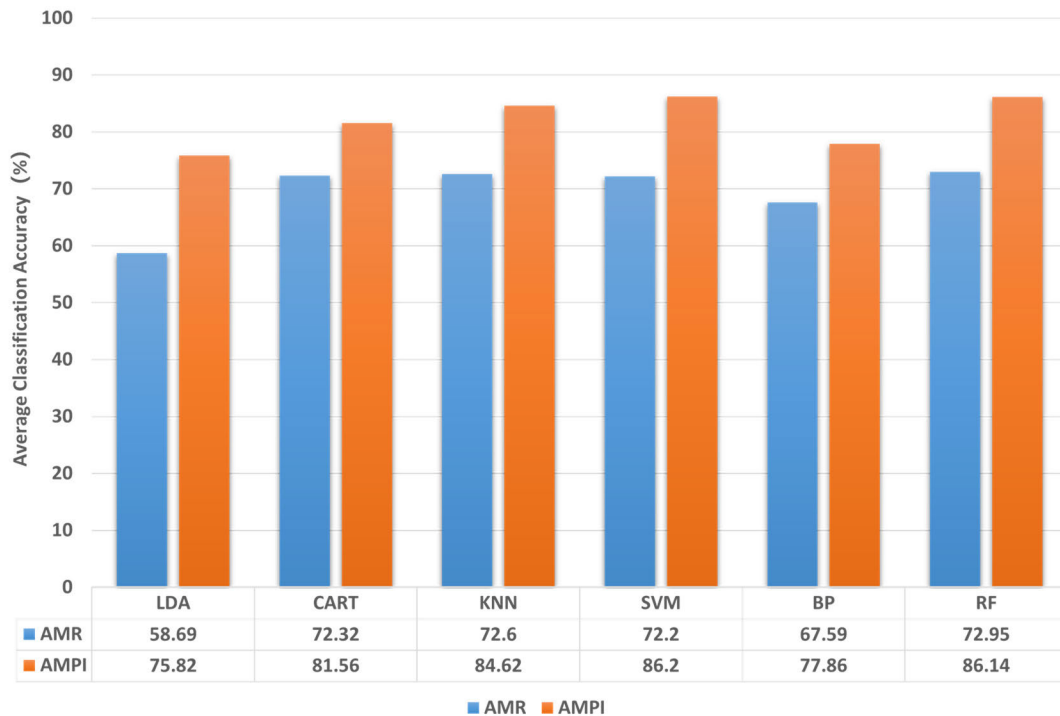


**FIGURE 7.** The average classification accuracy of the classification tests for activity muscle regions (AMR) and Active Muscle Position and Intensity (AMPI) by using six classifiers.

**TABLE 1.** Classification accuracy and average improvement rate for Each subject for activity muscle regions (AMR) and active muscle position and intensity (AMPI) by using SVM as classifier.

Subjects	AMR	AMPI	Average Growth Rate
Subject1	65.5%	84.4%	18.9%
Subject2	65.9%	84.3%	18.4%
Subject3	63.7%	90.1%	26.8%
Subject4	71.9%	91.9%	20.0%
Subject5	81.6%	91.1%	9.5%
Subject6	79.3%	88.5%	9.2%
Subject7	80.6%	92.6%	12.0%
Subject8	77.6%	91.3%	13.4%

Therefore, the final LZC is shown in (22).

$$LZC = \frac{C(n)}{b(n)} \quad (22)$$

## V. RESULTS AND DISCUSSION

Figure 7 shows the average classification accuracy of the classification tests for activity muscle regions (AMR) and active muscle position and intensity (AMPI) by using six classifiers. It is clear that active muscle position and intensity (AMPI) has better recognition. The high classification accuracy obtained shows that the new features can solve more challenging problems. As can be seen from the figure 6, the average improvement in classification accuracy for the six classifiers, namely linear discriminant Analysis (LDA), The

classification and regression tree (CART), k-nearest neighbor (KNN), support vector machine (SVM), back propagation neural network (BP) and random forest (RF) was 17.13%, 9.42%, 12.02%, 14.00%, 10.27% and 13.19% respectively. The results also show that SVM has the highest average classification accuracy on this data.

Table 1 shows the average classification accuracy and Average increase rate of the classification tests for Each subject for activity muscle regions (AMR) and active muscle position and intensity (AMPI) by using SVM as classifier. The difference in classification accuracy between the different subjects is due to differences in muscle anatomy. The variation in performance may also be due to differences in muscle contraction effort and muscle fatigue between the

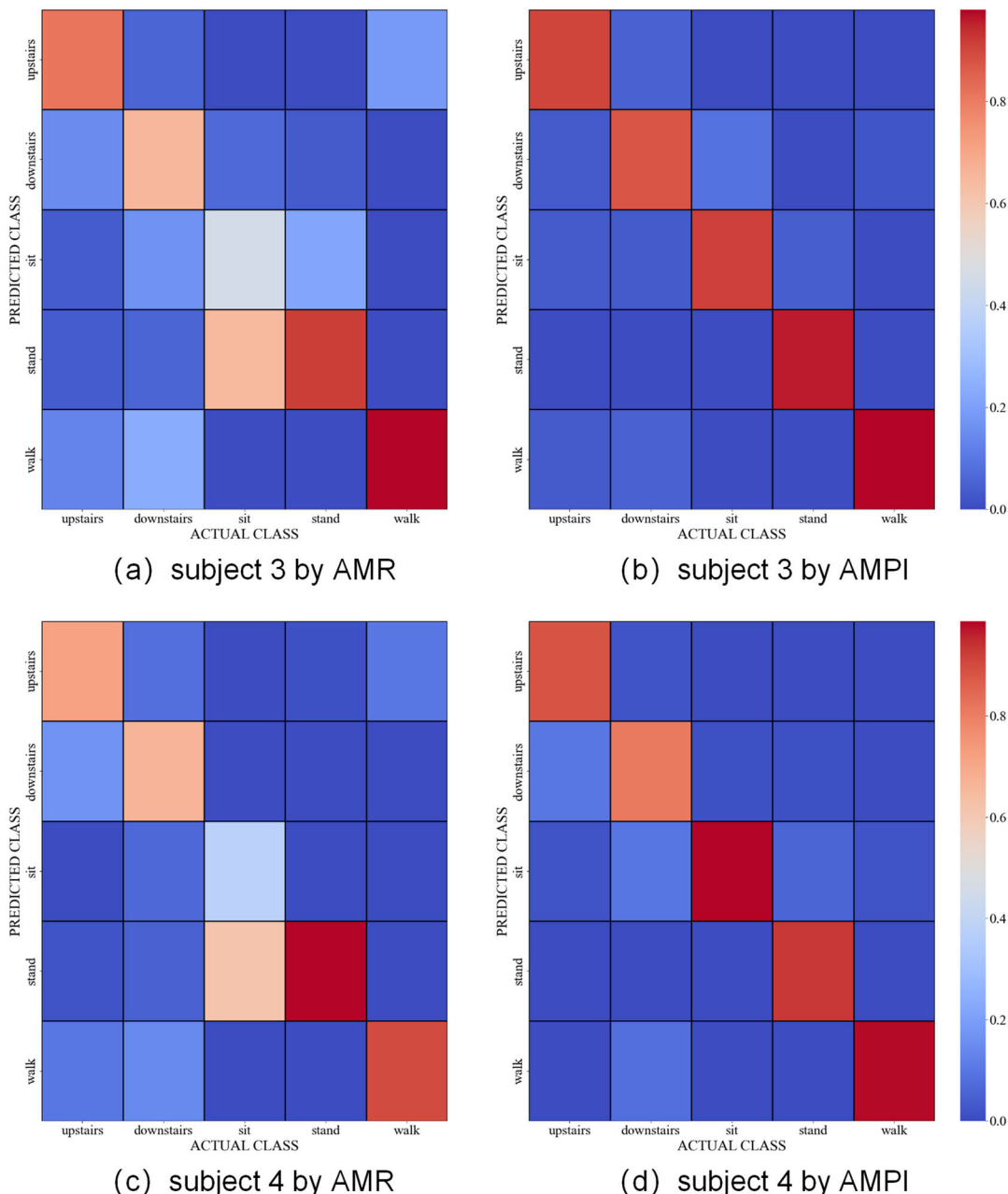


**FIGURE 8.** The confusion matrix showing class wise accuracy for five classes of leg movements for two subjects for activity muscle regions (AMR) and active muscle position and intensity (AMPI) by using SVM as classifier.

subjects. For all the eight subjects, the classification accuracy by using AMPI was higher than that by using AMR.

The confusion matrices for the two subjects using the SVM is shown in Figure 8. This is because SVM performs slightly better than other classifiers. As can be seen from the figure 8, there are difficulties in separating leg movements when using the AMR for classification, especially for two groups of movements: upstairs and downstairs, stand and sit. Because the two groups of movements are similar, and the joints and muscles used are also similar, it is difficult to distinguish when using the AMR for classification. This can be well

improved when using the improved feature, namely active muscle position and intensity (AMPI) for classification.

The confusion matrix of Figure 8 showing class wise accuracy for five classes of leg movements for two subjects for activity muscle regions (AMR) and active muscle position and intensity (AMPI) by using SVM as classifier.

For the investigation of different movement separability of the proposed AMPI, the confusion matrix across eight subjects was averaged. The average confusion matrix is as shown in Figure 9. For using the SVM as the classifier, it can be seen from the diagonal of the confusion matrix that the



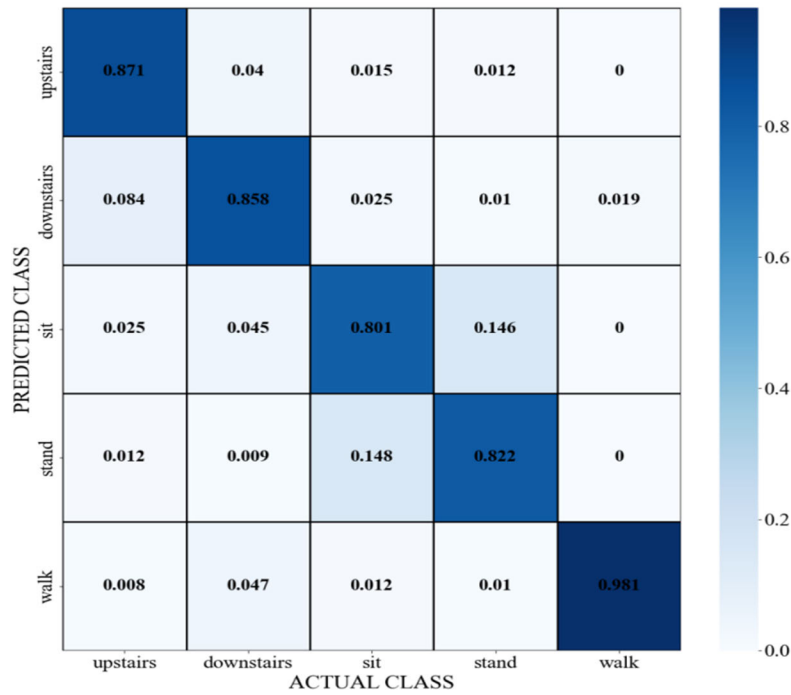


**FIGURE 9.** Average classification accuracy across eight subjects using SVM as a classifier after applying AMPI for classification of five classes of leg movements.

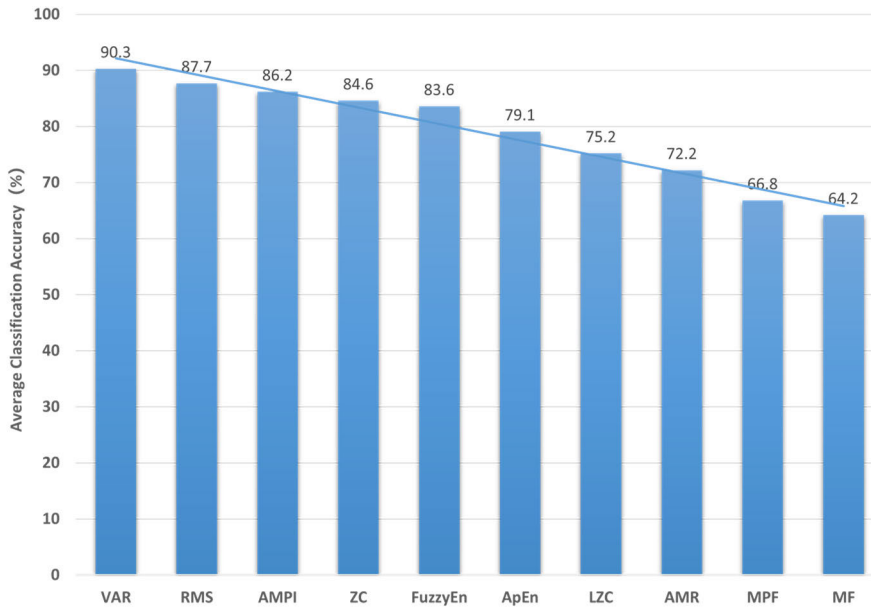


**FIGURE 10.** The Average classification accuracy of ten features.

classifier successfully classified five leg movement patterns. However, there are difficulties in separating stand and sit using SVM as classifier. The misclassification may be due to too similarity to the movement patterns. The maximum classification accuracy of AMPI was about 86.2% Using the SVM as a classifier. This seems acceptable in comparison to other work in the literature. The results also showed that

classification of five different leg movements using AMPI was successful.

Figure 10 shows the average classification accuracy of the classification test by the SVM classifier for AMPI, AMR and eight other traditional features. The main goal of this part is to make an overall assessment of the classification performance of the AMPI. By comparison, the new features

were found to be in the forefront of the ten features. It is only secondary to root mean square (RMS) and variance (VAR), and the average classification accuracy difference is very small, only 0.041 and 0.015. Moreover, AMPI has the highest classification accuracy compared with the commonly used frequency domain features and nonlinear features. This suggests that the new feature proposed in this study has great practical value in terms of pattern recognition.

## VI. CONCLUSION

This study presents an improved method for extracting sEMG features. When the pre-and post-improved sEMG features were compared using six common classifiers, the new features, namely active muscle position and intensity (AMPI), achieved the highest classification accuracy. Observing the confusion matrix shows that the new features classify similar actions better compared to activity muscle regions (AMR). This makes up for the biggest flaw of feature before improvement. The AMPI, AMR and the traditional eight sEMG features were tested for classification using SVM. The classification performance of the new features is in the top three and is higher than the common frequency domain features and non-linear features. This indicates that the AMPI has great utility in pattern recognition. Moreover, the new features retain the dimension reduction ability of the original features. As long as  $2r < N$  (where  $N$  is the number of channels and  $r$  is the number of selected active muscle), the feature dimension reduction can be realized, and the calculation cost and calculation time of the pattern recognition method can be reduced.

Future studies will use more channels and information to optimize and validate the new features. Apply the new features in more aspects, such as construction of a sEMG cloud map of the lower limbs, joint angle prediction, and so on. Ultimately, we want to achieve real-time control of lower limb exoskeleton robots based on sEMG. In addition, with the development of multi-channel sEMG acquisition equipment and the application of high-density electrodes, compared with the traditional time-frequency domain features, the AMPI based on active muscle areas will have greater utilization space and use value.

## REFERENCES

- [1] H. A. Varol, F. Sup, and M. Goldfarb, "Multiclass real-time intent recognition of a powered lower limb prosthesis," *IEEE Trans. Biomed. Eng.*, vol. 57, no. 3, pp. 542–551, Mar. 2010, doi: [10.1109/TBME.2009.2034734](https://doi.org/10.1109/TBME.2009.2034734).
- [2] H. Huang, F. Zhang, L. J. Hargrove, Z. Dou, D. R. Rogers, and K. B. Englehart, "Continuous locomotion-mode identification for prosthetic legs based on neuromuscular-mechanical fusion," *IEEE Trans. Biomed. Eng.*, vol. 58, no. 10, pp. 2867–2875, Oct. 2011, doi: [10.1109/TBME.2011.2161671](https://doi.org/10.1109/TBME.2011.2161671).
- [3] H. Huang, T. A. Kuiken, and R. D. Lipschutz, "A strategy for identifying locomotion modes using surface electromyography," *IEEE Trans. Biomed. Eng.*, vol. 56, no. 1, pp. 65–73, Jan. 2009, doi: [10.1109/TBME.2008.2003293](https://doi.org/10.1109/TBME.2008.2003293).
- [4] A. Phinyomark, P. Phukpattaranont, and C. Limsakul, "Fractal analysis features for weak and single-channel upper-limb EMG signals," *Exp. Syst. Appl.*, vol. 39, no. 12, pp. 11156–11163, Sep. 2012, doi: [10.1016/j.eswa.2012.03.039](https://doi.org/10.1016/j.eswa.2012.03.039).
- [5] J. Han, Q. Ding, A. Xiong, and X. Zhao, "A state-space EMG model for the estimation of continuous joint movements," *IEEE Trans. Ind. Electron.*, vol. 62, no. 7, pp. 4267–4275, Jul. 2015, doi: [10.1109/TIE.2014.2387337](https://doi.org/10.1109/TIE.2014.2387337).
- [6] D. Farina, I. Vujaklija, M. Sartori, T. Kapelner, F. Negro, N. Jiang, K. Bergmeister, A. Andalib, J. Principe, and O. C. Aszmann, "Man/machine interface based on the discharge timings of spinal motor neurons after targeted muscle reinnervation," *Nature Biomed. Eng.*, vol. 1, no. 2, p. 0025, Feb. 2017, doi: [10.1038/s41551-016-0025](https://doi.org/10.1038/s41551-016-0025).
- [7] C.-H. Wu, H.-F. Mao, J.-S. Hu, T.-Y. Wang, Y.-J. Tsai, and W.-L. Hsu, "The effects of gait training using powered lower limb exoskeleton robot on individuals with complete spinal cord injury," *J. NeuroEng. Rehabil.*, vol. 15, no. 1, pp. 1–10, Dec. 2018, doi: [10.1186/s12984-018-0355-1](https://doi.org/10.1186/s12984-018-0355-1).
- [8] G. Lv, Zhu and R. D. Gregg, "On the design and control of highly backdrivable lower-limb exoskeletons: A discussion of past and ongoing work," *IEEE Control Syst. Mag.*, vol. 38, no. 6, pp. 88–113, Dec. 2018, doi: [10.1109/MCS.2018.2866605](https://doi.org/10.1109/MCS.2018.2866605).
- [9] D. R. Louie, W. B. Mortenson, M. Durocher, R. Teasell, J. Yao, and J. J. Eng, "Exoskeleton for post-stroke recovery of ambulation (ExStRA): Study protocol for a mixed-methods study investigating the efficacy and acceptance of an exoskeleton-based physical therapy program during stroke inpatient rehabilitation," *BMC Neurol.*, vol. 20, no. 1, pp. 1–9, Dec. 2020, doi: [10.1186/s12883-020-1617-7](https://doi.org/10.1186/s12883-020-1617-7).
- [10] H. Kazerooni, R. Steger, and L. Huang, "Hybrid control of the Berkeley lower extremity exoskeleton (BLEEX)," *Int. J. Robot. Res.*, vol. 25, nos. 5–6, pp. 561–573, 2006, doi: [10.1177/0278364906065505](https://doi.org/10.1177/0278364906065505).
- [11] A. Esquenazi, M. Talaty, A. Packel, and M. Saulino, "The ReWalk powered exoskeleton to restore ambulatory function to individuals with thoracic-level motor-complete spinal cord injury," *Amer. J. Phys. Med. Rehabil.*, vol. 91, no. 11, pp. 911–921, 2012, doi: [10.1097/PHM.0b013e318269d9a3](https://doi.org/10.1097/PHM.0b013e318269d9a3).
- [12] S. Yu, H. Lee, W. Kim, and C. Han, "Development of an underactuated exoskeleton for effective walking and load-carrying assist," *Adv. Robot.*, vol. 30, no. 8, pp. 535–551, Apr. 2016, doi: [10.1080/01691864.2015.1135080](https://doi.org/10.1080/01691864.2015.1135080).
- [13] E. C. Lovasz, D. T. Margineanu, V. Ciupe, I. Maniu, C. M. Guescu, E. S. Zabava, and S. D. Stan, "Design and control solutions for haptic elbow exoskeleton module used in space telerobotics," *Mech. Mach. Theory*, vol. 107, pp. 384–398, Jan. 2017, doi: [10.1016/j.mechmachtheory.2016.08.004](https://doi.org/10.1016/j.mechmachtheory.2016.08.004).
- [14] A. Phinyomark, P. Phukpattaranont, and C. Limsakul, "Feature reduction and selection for EMG signal classification," *Exp. Syst. Appl.*, vol. 39, no. 8, pp. 7420–7431, Jun. 2012, doi: [10.1016/j.eswa.2012.01.102](https://doi.org/10.1016/j.eswa.2012.01.102).
- [15] T. Tuncer, S. Dogan, and A. Subasi, "Surface EMG signal classification using ternary pattern and discrete wavelet transform based feature extraction for hand movement recognition," *Biomed. Signal Process. Control*, vol. 58, Apr. 2020, Art. no. 101872, doi: [10.1016/j.bspc.2020.101872](https://doi.org/10.1016/j.bspc.2020.101872).
- [16] V. Shanmuganathan, H. R. Yesudhas, M. S. Khan, M. Khari, and A. H. Gandomi, "R-CNN and wavelet feature extraction for hand gesture recognition with EMG signals," *Neural Comput. Appl.*, vol. 32, no. 21, pp. 16723–16736, Nov. 2020, doi: [10.1007/s00521-020-05349-w](https://doi.org/10.1007/s00521-020-05349-w).
- [17] O. S. Powar, K. Chemmangat, and S. Figarado, "A novel pre-processing procedure for enhanced feature extraction and characterization of electromyogram signals," *Biomed. Signal Process. Control*, vol. 42, pp. 277–286, Apr. 2018, doi: [10.1016/j.bspc.2018.02.006](https://doi.org/10.1016/j.bspc.2018.02.006).
- [18] L. Ge, L.-J. Ge, and J. Hu, "Feature extraction and classification of hand movements surface electromyogram signals based on multi-method integration," *Neural Process. Lett.*, vol. 49, no. 3, pp. 1179–1188, Jun. 2019, doi: [10.1007/s11063-018-9862-0](https://doi.org/10.1007/s11063-018-9862-0).
- [19] X. Xi, W. Jiang, S. M. Miran, X. Hua, Y. Zhao, C. Yang, and Z. Luo, "Feature extraction of surface electromyography based on improved small-world leaky echo state network," *Neural Comput.*, vol. 32, no. 4, pp. 741–758, Apr. 2020, doi: [10.1162/neco\\_a\\_01270](https://doi.org/10.1162/neco_a_01270).
- [20] G. Li, J. Li, Z. Ju, Y. Sun, and J. Kong, "A novel feature extraction method for machine learning based on surface electromyography from healthy brain," *Neural Comput. Appl.*, vol. 31, no. 12, pp. 9013–9022, Dec. 2019, doi: [10.1007/s00521-019-04147-3](https://doi.org/10.1007/s00521-019-04147-3).
- [21] L. Hargrove, K. Englehart, and B. Hudgins, "A training strategy to reduce classification degradation due to electrode displacements in pattern recognition based myoelectric control," *Biomed. Signal Process. Control*, vol. 3, no. 2, pp. 175–180, Apr. 2008, doi: [10.1016/j.bspc.2007.11.005](https://doi.org/10.1016/j.bspc.2007.11.005).
- [22] L. Ren, C. Wang, J. Fang, J. Tian, and J. Zhou, "Research on key technology of feature extraction based on surface EMG," in *Proc. Int. Conf. Algorithms, Microchips Netw. Appl.*, May 2022, Art. no. 1217618.

- [23] J. Maier, A. Naber, and M. Ortiz-Catalan, "Improved prosthetic control based on myoelectric pattern recognition via wavelet-based de-noising," *IEEE Trans. Neural Syst. Rehabil. Eng.*, vol. 26, no. 2, pp. 506–514, Feb. 2018, doi: [10.1109/TNSRE.2017.2771273](https://doi.org/10.1109/TNSRE.2017.2771273).
- [24] F. Khateb, P. Prommee, and T. Kulej, "MIOTA-based filters for noise and motion artifact reductions in biosignal acquisition," *IEEE Access*, vol. 10, pp. 14325–14338, 2022, doi: [10.1109/ACCESS.2022.3147665](https://doi.org/10.1109/ACCESS.2022.3147665).
- [25] Y. Zhou, C. Chen, M. Cheng, Y. Alshahrani, S. Franovic, E. Lau, G. Xu, G. Ni, J. M. Cavanaugh, S. Muh, and S. Lemos, "Comparison of machine learning methods in sEMG signal processing for shoulder motion recognition," *Biomed. Signal Process. Control*, vol. 68, Jul. 2021, Art. no. 102577, doi: [10.1016/j.bspc.2021.102577](https://doi.org/10.1016/j.bspc.2021.102577).
- [26] L. Liu, P. Liu, E. A. Clancy, E. Scheme, and K. B. Englehart, "Electromyogram whitening for improved classification accuracy in upper limb prosthesis control," *IEEE Trans. Neural Syst. Rehabil. Eng.*, vol. 21, no. 5, pp. 767–774, Sep. 2013, doi: [10.1109/TNSRE.2013.2243470](https://doi.org/10.1109/TNSRE.2013.2243470).
- [27] Y. Zhao, J. Pei, and H. Chen, "Multi-layer radial basis function neural network based on multi-scale kernel learning," *Appl. Soft Comput.*, vol. 82, Sep. 2019, Art. no. 105541, doi: [10.1016/j.asoc.2019.105541](https://doi.org/10.1016/j.asoc.2019.105541).
- [28] B. Mor, S. Garhwal, and A. Kumar, "A systematic review of hidden Markov models and their applications," *Arch. Comput. Methods Eng.*, vol. 28, no. 3, pp. 1429–1448, May 2021, doi: [10.1007/s11831-020-09422-4](https://doi.org/10.1007/s11831-020-09422-4).
- [29] A. Furui, H. Hayashi, and T. Tsuji, "A scale mixture-based stochastic model of surface EMG signals with variable variances," *IEEE Trans. Biomed. Eng.*, vol. 66, no. 10, pp. 2780–2788, Oct. 2019, doi: [10.1109/TBME.2019.2895683](https://doi.org/10.1109/TBME.2019.2895683).
- [30] A. M. Vögele, R. R. Zsoldos, B. Kruger, and T. Licka, "Novel methods for surface EMG analysis and exploration based on multi-modal Gaussian mixture models," *PLoS ONE*, vol. 11, no. 6, Jun. 2016, Art. no. e0157239, doi: [10.1371/journal.pone.0157239](https://doi.org/10.1371/journal.pone.0157239).
- [31] D. Jiang, G. Li, Y. Sun, J. Kong, B. Tao, and D. Chen, "Grip strength forecast and rehabilitative guidance based on adaptive neural fuzzy inference system using sEMG," *Pers. Ubiquitous Comput.*, vol. 26, no. 4, pp. 1215–1224, Aug. 2022, doi: [10.1007/s00779-019-01268-3](https://doi.org/10.1007/s00779-019-01268-3).
- [32] L. Zhang and W. Zhou, "Fisher-regularized support vector machine," *Inf. Sci.*, vol. 343, pp. 79–93, May 2016, doi: [10.1016/j.ins.2016.01.053](https://doi.org/10.1016/j.ins.2016.01.053).



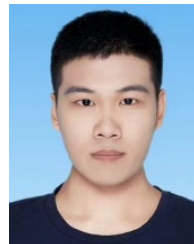
**LUYAO MA** received the B.S. degree in mechanical engineering from Xinjiang University, Xinjiang, China, in 2021, where she is currently pursuing the Ph.D. degree in mechanical engineering. Her current research interests include biomedical signal decoding, pattern recognition, joint angle prediction and their applications to exoskeleton systems, and rehabilitation robot systems.



**QING TAO** received the M.Sc. degree from the Huazhong University of Science and Technology, China, in 2003, and the Ph.D. degree from Xinjiang University, China. He is currently a Professor and the Dean of the School of Mechanical Engineering, Xinjiang University. His research interests include mechanical design, human modeling and simulation, industrial design, and rehabilitation robots.



**QINGZHENG CHEN** received the B.S. degree in engineering from the South China University of Technology, Hunan, China, in 2019, and the master's degree in mechanical engineering from Xinjiang University, Xinjiang, China, in 2022, where he is currently pursuing the Ph.D. degree in mechanical engineering. His research interests include rehabilitation robotics motion control techniques, biosignal processing techniques, pattern recognition, and deep learning.



**ZIRUI ZHAO** was born in Zibo, Shandong, in 1997. He received the B.S. degree in engineering from the School of Mechanical Engineering, Shijiazhuang Railway University, in 2020. He is currently pursuing the master's degree in mechanical engineering with Xinjiang University. His research interests include physiological electrical signal processing, pattern recognition technology, and quantitative evaluation of lower limb rehabilitation.

...